

## Phase separation and droplet nucleation induced by an optical piston

J. P. Delville, C. Lalaude, E. Freysz, and A. Ducasse

*Centre de Physique Moléculaire Optique et Hertzienne, Université Bordeaux I, 351 Cours de la Libération,  
F-33405 Talence Cedex, France*

(Received 15 January 1993)

We propose to use laser-induced concentration variations due to electrostrictive or thermodiffusive coupling in order to drive a phase separation in a liquid mixture. The properties of such a composition quench, analyzed in a microemulsion in the thermodiffusive case, are reported. Droplets of the minority phase are nucleated and trapped in the laser beam, and their dynamics is described. This experiment allows one to analyze nucleation in an original wetting-free one-dimensional geometry.

PACS number(s): 64.70.Ja, 05.70.Fh, 42.65.Jx, 82.70.Kj

In the last few years, phase separation processes have been extensively analyzed from both theoretical and experimental viewpoints [1]. Generally, dynamics and pattern evolutions of phase separation in liquid mixtures are strongly dependent on quench conditions and on geometrical confinement of the medium. Thus, different phase separation behaviors are expected according to the type of quench procedure, which can involve variations of temperature, pressure [2], or composition. However, to our knowledge, no quench induced by composition variations has so far been reported. On the other hand, the domain growth is strongly influenced by gravity-induced flows occurring in the bulk, which increase the complexity of the pattern dynamics. In classical walls-confined geometry, this problem is partially eliminated but wetting processes start playing a crucial role [3]. In confined geometry avoiding the presence of walls, original behaviors are then expected and deserve to be analyzed. Laser-induced phase separation could lead to such a situation.

Since the pioneer work of Ashkin on trapping and levitation of particles with a strongly focused laser beam [4], it has been shown that laser waves are able to locally modulate the particle density and hence to change the composition of any mixture whose components have different refractive indices [5]. Physically two different mechanisms account for such concentration variations. The first one is due to electrostrictive forces, which originate from the coupling of the dipole moment induced by the field on each particle, with the gradient of this field [6]. Besides, even a small wave-generated temperature gradient results in a concentration gradient due to thermodiffusion [7]. These concentration variations, which are responsible of large optical nonlinearities in some systems [8], could also allow one to induce phase transitions in a one-dimensional (1D) confined geometry. We describe in this work this laser-induced quench in composition and we analyze the resulting phase separation in a micellar phase of microemulsion.

A simple description of this type of transition induced by low power lasers can be obtained by considering the interaction of the wave with a binary liquid system. We

assume a mixture initially located close to a coexistence curve in the one-phase part of the phase diagram, as shown in Fig. 1. Its evolution in the presence of the wave is presented in the plane  $(C, \Pi)$  where  $C$  is the concentration of one of the components and  $\Pi$  the osmotic pressure.  $C_0$  and  $T_0$  are the initial concentration and temperature. It is assumed afterwards that the absorption  $\alpha_a$  of the liquid is very small at the used optical wavelength, in such a way that the laser-induced temperature variation  $\delta T$  can be neglected when one describes the wave-medium interaction in the phase diagram. Thus, far enough from the critical point, the followed path is considered as isothermal.

The wave interacting with the medium is a Gaussian cw laser beam propagating along the  $z$  axis. Its intensity can be written in the following form (TEM<sub>00</sub> mode):

$$|E(r, z)|^2 = \frac{8}{c_1 \sqrt{\epsilon_L}} \frac{P(z)}{a^2(z)} \exp \left[ -\frac{r^2}{a^2(z)} \right], \quad (1)$$

$r$  is the transverse distance to the  $z$  axis,  $P(z)$  the beam power,  $a(z)$  the beam radius,  $c_1$  the light velocity in vac-

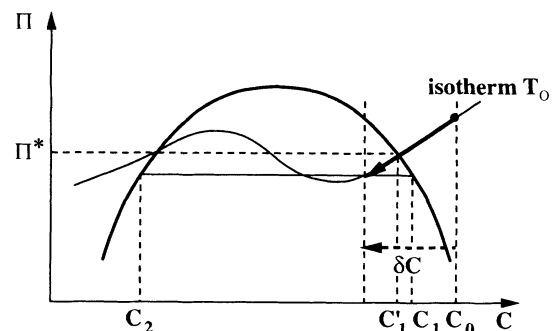


FIG. 1. Phase coexistence of a binary liquid mixture.  $C$  is the concentration of one of the components and  $\Pi$  is the osmotic pressure.  $\Pi^*$  corresponds to the Maxwell plateau value at the temperature  $T_0$ .  $\delta C$  represents the isothermal optical quenching in the metastable region from the initial one-phase state of concentration  $C_0$ .

uum, and  $\epsilon_L$  the linear dielectric constant of the mixture. The gradient of this field results in a variation  $\delta C(r, z)$  of the concentration via both electrostrictive and thermodiffusive processes [8]. The electrostrictive contribution is proportional to the field intensity  $|E|^2$  and to the osmotic compressibility  $K_T$ . Thermodiffusion is related to the temperature gradient  $\nabla \delta T(r, z)$  induced by the wave. If the transverse size of the cell containing the mixture is very large compared to the beam radius and assuming a cylindrical symmetry around  $z$ ,  $\delta T(r, z)$  can be written as [9]

$$\delta T(r, z) = B_1 P(z) u \left[ \frac{r^2}{a^2(z)} \right] \quad (2)$$

with  $B_1 = \alpha_a / \pi \Lambda$ , where  $\Lambda$  is the thermal conductivity,  $u(r^2/a^2(z))$  is a function depending on the thermal boundary conditions in the cell. The thermodiffusive contribution to  $\delta C$  is proportional to  $\delta T$  and to the thermodiffusive constant  $k_T$  [10]. It is important to note that, even if the amplitude of  $\delta T$  is too weak to result in a noticeable moving of the representative point in the phase diagram, the corresponding thermodiffusive contribution to  $\delta C$  can lead to a large displacement for mixtures characterized by large  $k_T$  values. In the stationary limit, the total  $\delta C$  variation is [8]

$$\delta C(r, z) = B_2 K_T |E(r, z)|^2 - B_1 \frac{k_T}{T_0} P(z) u \left[ \frac{r^2}{a^2(z)} \right] \quad (3)$$

with  $B_2 = C_0^2 (\partial \epsilon_L / \partial C) / 8 \pi \rho_0$ , where  $\rho_0$  is the initial density. As shown in Fig. 1,  $\delta C$  results in a local variation of the osmotic pressure  $\delta \Pi \approx (1/K_T C_0) \delta C$ . Then, besides the classical laser-induced heating [11], this laser-induced osmotic piston effect is an original tool to induce a phase separation. Each contribution of  $\delta C$  can be positive or negative since the sign of  $(\partial \epsilon_L / \partial C)$  depends on the relative dielectric constant of the two components and  $k_T$  can be positive or negative according to the chosen mixture [10]. We have assumed in Fig. 1 a negative value of  $\delta C$  corresponding to  $(\partial \epsilon_L / \partial C) < 0$  and  $k_T > 0$ . If  $|\delta C| > |\delta C^*| = |C_1 - C_0|$ , Fig. 1 shows that the wave interaction leads to an isothermal quench in composition in the metastable region. Due to fluctuations, this quench results in a local phase separation by nucleation and growth processes [1].

The experimental setup is presented in Fig. 2. The analyzed mixture is contained in a temperature-controlled optical fused quartz cell (2 mm thick, 1 cm wide) placed at the focal point of a  $\times 10$  microscope objective  $L_1$  which focuses a cw  $\text{Ar}^+$  laser beam ( $\lambda = 5145 \text{ \AA}$ ) at the entrance plane face of the cell ( $z = 0$ ). We visualize the location of the beam-waist  $a_0$  [i.e.,  $a(z=0) = a_0$ ] inside the cell and record the evolution of the interaction along the laser beam by means of an optical system composed of a lens and a charge-coupled-device (CCD) video camera coupled to a video screen. Values of  $a_0$  ranging from 2–8  $\mu\text{m}$  can be achieved by varying the optical path between the two lenses  $L_1$  and  $L_2$  ( $f_2 = 20 \text{ cm}$ ).

The analyzed liquid medium is a quaternary mixture of water, oil, surfactant (soap), and cosurfactant (alcohol)

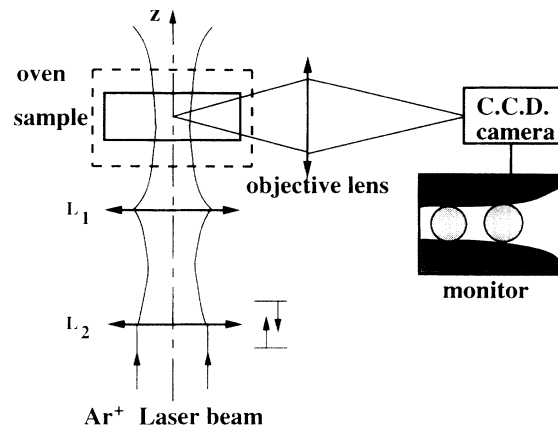


FIG. 2. Experimental setup.

with the following mass composition: water 5%, *n*-dodecane 78%, sodium dodecyl sulfate 4.8%, and *n*-pentanol 12.2%. It features at room temperature a micellar structure: the water forms a stable suspension of spherical droplets of eight nanometers in diameter (called micelles), isolated from the oil (dodecane) by a shell of amphiphilic molecules. This particular composition has been chosen because it is located close to a coexistence curve between a high critical temperature ( $T_c \approx 32^\circ\text{C}$ ) and a low demixion temperature ( $T_d \approx 20^\circ\text{C}$ ) such that a very small decrease of the micellar concentration induces a liquid-liquid phase separation towards a lower micellar concentration phase [12]. The volume fraction of micelles of the initial micellar phase is  $\phi_0 = 0.11$ , and the mean value of its refractive index is  $n_L = 1.4148$ . It has been calculated from the Clausius-Mossotti relation involving the index  $n_d = 1.3914$  of the dispersed phase (the micelles) and the index  $n_c = 1.4174$  of the continuous oil phase [13]. The absorption coefficient value at  $\lambda = 5145 \text{ \AA}$ , measured by an interferometric method at room temperature, is  $\alpha_a = 5.58 \times 10^{-4} \text{ cm}^{-1}$  [14] and the thermal conductivity is  $\Lambda = 1.45 \times 10^{-3} \text{ W cm}^{-1} \text{ K}^{-1}$  [15].

According to the phase diagram [12], a very small concentration change  $\delta C^*$  evaluated to be  $-4 \times 10^{-3}$  in the beam center at  $T_0 = 298 \text{ K}$ , is required to induce the phase separation. Experimentally, a laser-beam power  $P_0 \geq P^*$  of the order of 100 mW fulfills this requirement [i.e.,  $\delta C(P^*) = \delta C^*$ ] [16]. In our case, the thickness of the cell ( $l = 2 \text{ mm}$ ) is always large compared to the beam radius. Thus, wetting phenomena do not affect the morphology of the phase separation induced by the field. The optical quench in the metastable two-phase region results in the nucleation inside the beam of droplets constituted by the minority phase. This is illustrated in Fig. 3. A laser beam of power  $P_0 = 0.11 \text{ W}$  with a beam-waist  $a_0 = 6 \mu\text{m}$  propagates inside the sample at room temperature  $T_0 = 298 \text{ K}$ . The condition  $P_0 \geq P^*$  is fulfilled and the quench in composition is observed.

Since  $\Delta \epsilon_L \approx (\partial \epsilon_L / \partial C)(C_2 - C_1)$  and both  $(\partial \epsilon_L / \partial C) \approx -5.69 \times 10^{-2}$  and  $(C_2 - C_1)$  are negative, the refractive index of the nucleated droplets is larger than that of the surrounding phase. Because the droplet polarisability  $p_d$  is proportional to its volume, here of the order of few

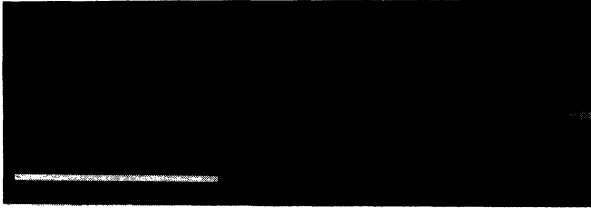


FIG. 3. Beam trapping of the nucleated droplets and laser beam self-focusing resulting from their converging ball lens effect. The left part of the photograph corresponds to the entrance face of the cell. The successive droplets observed along the beam axis have been nucleated consecutively in time. This explains why the droplets are larger and larger from left to right. The values of the control parameters are:  $a_0=6 \mu\text{m}$ ,  $P_0=0.22 \text{ W}$ ,  $T_0=298 \text{ K}$ . The bar corresponds to  $100 \mu\text{m}$ .

hundreds of  $\mu\text{m}^3$ , the electrostrictive energy  $W = -\frac{1}{2}p_d|E|^2$  is large compared to the Boltzmann energy  $k_B T_0$ : at room temperature  $|W|/k_B T_0 \approx 3.10^3$  for a droplet radius  $r_d \approx a_0 = 5 \mu\text{m}$  and a beam power  $P_0 = 0.1 \text{ W}$ . As a consequence the electrostrictive forces move the droplets towards the beam center. The resulting optical trapping is illustrated in Fig. 3 which also shows that the droplets self-trap in turn the laser beam. Each droplet acts as a lens of a spherical shape (ball lens). The medium behaves as a set of self-induced ball lenses that focuses the laser beam. This self-focusing process [16,17] leads to other original droplet nucleation dynamics. The most usual scenario can be described as follows. Around the new beam-waist generated by the lens effect of the first droplet, the conditions of homogeneous nucleation are satisfied again. A new droplet is then nucleated. It grows inside the beam, focuses light, induces another beam-waist, and so on. Figure 4 illustrates this mechanism. At the focal point generated by the large droplet, a set of very small beam-trapped droplets (pointed by an arrow) is nucleated.

Our quenching method allows us to observe the dynamics of the induced-phase separation. As soon as the field is applied, one can directly analyze the droplet growth with the CCD video camera. In fact, in these experiments, a new type of one-dimensional (1D) confined geometry of nucleation, different from those previously

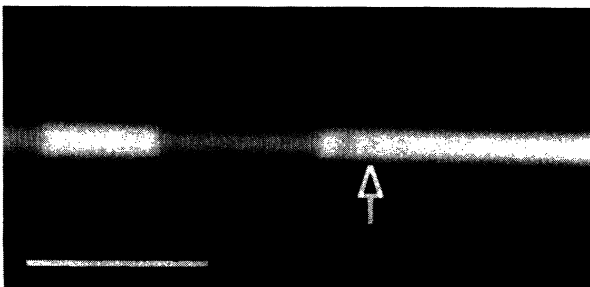


FIG. 4. Homogeneous nucleation of a set of very small droplets (pointed by the arrow) induced at the intermediate beam-waist resulting from the lens effect of the nearest beam-trapped droplet. The values of the control parameters are:  $a_0=6 \mu\text{m}$ ,  $P_0=0.22 \text{ W}$ ,  $T_0=298 \text{ K}$ . The bar corresponds to  $50 \mu\text{m}$ .

analyzed in thermal quenching [3] and in breath figures [18], is created. Original behaviors are observed. Since no substrate or no capillary is needed to localize the nucleation along an axis in the bulk, wetting processes are completely eliminated. Moreover, the free moving of the droplets along the beam axis strongly reduces the 1D interactions resulting in coalescence between large droplets [19]. Finally, it has to be noted that the longitudinal optical radiation pressure and the gravity coupling, which could strongly modify these interactions and the droplet growth, are very weak in our case due to the small contrasts of dielectric constant and density: at room temperature  $\Delta\epsilon_L \approx 1.3 \times 10^{-2}$ ,  $\Delta\rho_L \approx -3.10^{-2} \text{ g/cm}^3$ . The droplet velocity along the beam axis resulting from the sum of both contributions (the beam is directed towards the ascendant vertical and the droplets have a lower density than the surrounding phase) can be computed in the Rayleigh-Gans approximation. The Stokes law leads to a very weak value  $V_d \approx 40 \mu\text{m/min}$  for an isolated droplet of radius  $r_d = 5 \mu\text{m}$ , which is in quite good agreement with the measured one. As a consequence, after an optical quench in the metastable region, the droplet growth is essentially controlled by that of an individual droplet:  $r_d = At^\beta$ , where  $A$  is the amplitude prefactor and  $\beta = \frac{1}{3}$ .

Figure 5 shows an experimental growth law obtained for a laser-beam power  $P_0 = 0.11 \text{ W}$  with a beam-waist  $a_0 = 7 \mu\text{m}$  at the temperature  $T_0 = 24.5^\circ\text{C}$ . The slope of the linear least-squares regression yields a growth exponent  $\beta = 0.28$  and an amplitude  $A = 2.35 \mu\text{m s}^{-\beta}$ . It is convenient to express  $r_d$  and  $t$  in dimensionless form to compare these experimental results with predicted growth rates [1,2]. In this case, the correlation length of density fluctuations in the two-phase region,  $\xi^-(T_0) = \xi_0^- ((T_c - T_0)/(T_c))^{-\nu}$  with  $\nu = 0.63$ , and the associated relaxation time,  $\tau^- = 6\pi\eta(\xi^-)^3/k_B T_0$ , where  $\eta$  is the shear viscosity, are, respectively, the relevant length and time scales. It has been shown that the behavior of the scaled wave number  $K^* = 2\pi\xi^-/r_d$  as a function of  $\tau^* = t/\tau^-$  has a universal behavior described

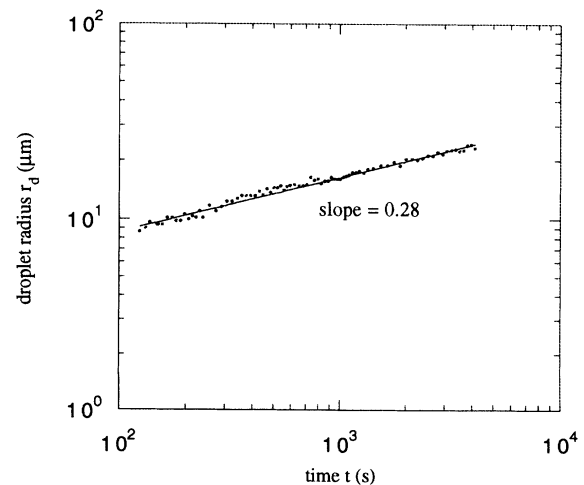


FIG. 5. Experimental growth law of one beam-trapped droplet fitted linearly in doubly logarithmic scales. The values of the control parameters are:  $a_0=7 \mu\text{m}$ ,  $P_0=0.11 \text{ W}$ ,  $T_0=297.5 \text{ K}$ .

by the equation  $K^* = K_0(\tau^*)^{-\beta}$  [20]. From the physical parameters  $\xi_0^- = 11 \text{ \AA}$  [12] and  $\eta \approx 3.41 \times 10^{-3} \text{ Pa s}$  [16] one gets  $K_0 \approx 0.62$  at  $T_0 = 297.5 \text{ K}$ , in good agreement with theoretical predictions [20].

We finally focus on the mechanism inducing the quench in composition. In order to evaluate the thermodiffusive concentration variation  $(\delta C)_{\text{th}}$  [i.e.,  $(\delta C)_{\text{th}} = -(k_T/T_0)\delta T$ ], we have computed the laser-induced temperature variation. For a laser-beam power  $P_0 = 0.1 \text{ W}$  with a  $5\text{-}\mu\text{m}$  beam-waist, one finds  $\delta T(r=0) \approx 4.4 \times 10^{-2} \text{ }^\circ\text{C}$ . This very small temperature increase justifies that the medium evolution can be considered as isothermal far enough from the critical point. The thermodiffusive constant  $k_T^0$  is unknown for this particular microemulsion [ $k_T = k_T^0((T_C - T_0)/T_C)^{-\gamma}$ ]. However, from comparison with a similar micellar system [7] and arguments upon the medium structure [17], we can assume  $k_T^0 \approx 4$ . One finds then  $(\delta C)_{\text{th}}(r=0) \approx -6 \times 10^{-3}$  in the beam center at  $T_0 = 298 \text{ K}$ , a value that can easily explain the observed laser-induced phase separation by a thermodiffusive process. On the other hand, the electrostrictive contribution  $(\delta C)_{\text{elec}}$  [i.e.,  $(\delta C)_{\text{elec}} = B_2 K_T |E|^2$ ] is negligible compared to the previous one. According to [5],  $(\delta C)_{\text{elec}}/C_0$

$\approx \frac{1}{2} p_{\text{mic}} |E|^2 \phi_0 K_T / v_{\text{mic}}$ , where  $v_{\text{mic}}$  is the volume of a micelle and  $p_{\text{mic}}$  its polarizability. Since  $\phi_0 K_T / v_{\text{mic}} \approx 1/k_B T_0 [(T_C - T_0)/T_0]^{-\gamma}$ , where  $\gamma = 1.24$ , one finds in the same experimental conditions  $(\delta C)_{\text{elec}}(r=0) \approx -2 \cdot 10^{-4}$ , a value that is an order of magnitude smaller than  $\delta C^*$ .

In conclusion, we have demonstrated the efficiency of a laser beam as an osmotic piston for driving a phase separation in a liquid mixture. For our particular medium the quench in composition is induced by thermodiffusion. Since the field creates a perturbation strongly localized in space, this optical quench results in a new type of 1D confined phase separation. The generalization of this process to other mixtures (especially in microemulsions in which electrostriction is dominant [5]) and a detailed description of the droplet growth are actually in progress.

We are grateful to A. M. Bellocq and Y. Garrabos for helpful discussions and to M. Maugey and J. Plantard for technical assistance. This work was partly supported by the Ministère de la Recherche et de l'Espace. The Centre de Physique Moléculaire Optique et Hertzienne is "associé au Centre National de la Recherche Scientifique."

- 
- [1] J. D. Gunton, M. San Miguel, and P. S. Sahni, in *Phase Transition and Critical Phenomena*, edited by C. Domb and J. L. Lebowitz (Academic, New York, 1983), Vol. 8.
- [2] N. C. Wong and C. M. Knobler, *J. Chem. Phys.* **69**, 725 (1978).
- [3] H. Tanaka, *Phys. Rev. Lett.* **70**, 53 (1993); **70**, 2770 (1993).
- [4] A. Ashkin, *Phys. Rev. Lett.* **24**, 156 (1970).
- [5] E. Freysz *et al.*, *J. Phys. Lett.* **46**, L-181 (1985).
- [6] A. J. Palmer, *Opt. Lett.* **5**, 54 (1980).
- [7] B. Jean-Jean *et al.*, *Europhys. Lett.* **7**, 219 (1988).
- [8] B. Jean-Jean *et al.*, *Phys. Rev. A* **39**, 5268 (1989).
- [9] J. P. Gordon *et al.*, *J. Appl. Phys.* **36**, 3 (1965).
- [10] M. Giglio and A. Vendramini, *Phys. Rev. Lett.* **34**, 561 (1975); **38**, 26 (1977).
- [11] I. Janossy, M. R. Taghizadeh, and E. Abraham in *Optical Bistability III*, edited by H. M. Gibbs *et al.* (Springer-Verlag, Berlin, 1986).
- [12] D. Gazeau *et al.*, *Europhys. Lett.* **9**, 833 (1989).
- [13] N. Rebbouh and J. R. Lalanne, *J. Chem. Phys.* **90**, 1175 (1989).
- [14] L. Canioni, L. Sarger, and P. Segonds (private communication).
- [15] P. Dorion *et al.*, *J. Chem. Phys.* **87**, 578 (1987).
- [16] A. Ponton *et al.*, *Europhys. Lett.* **17**, 27 (1992).
- [17] J. P. Delville, Ph.D. thesis, Université de Bordeaux, 1992.
- [18] A. Steyer *et al.*, *Europhys. Lett.* **12**, 211 (1990).
- [19] A. Steyer *et al.*, *Phys. Rev. B* **42**, 1086 (1990).
- [20] Y. Garrabos *et al.*, *Europhys. Lett.* **19**, 491 (1992).

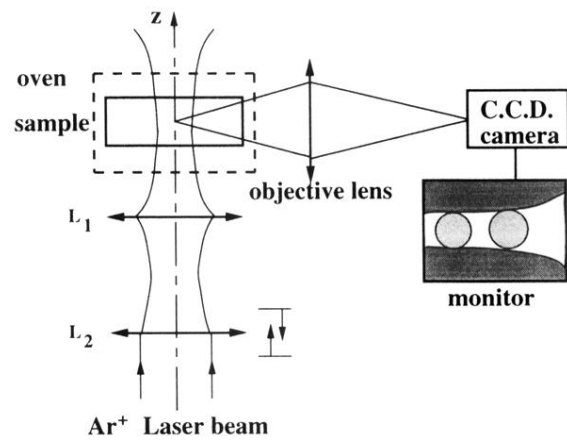


FIG. 2. Experimental setup.

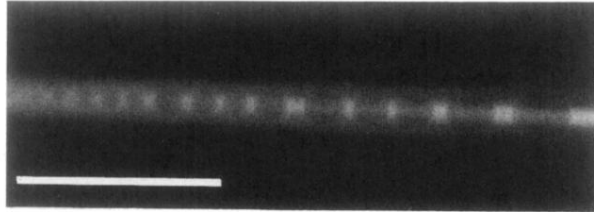


FIG. 3. Beam trapping of the nucleated droplets and laser beam self-focusing resulting from their converging ball lens effect. The left part of the photograph corresponds to the entrance face of the cell. The successive droplets observed along the beam axis have been nucleated consecutively in time. This explains why the droplets are larger and larger from left to right. The values of the control parameters are:  $a_0=6 \mu\text{m}$ ,  $P_0=0.22 \text{ W}$ ,  $T_0=298 \text{ K}$ . The bar corresponds to  $100 \mu\text{m}$ .

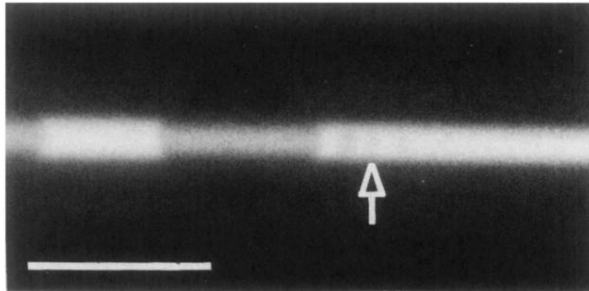


FIG. 4. Homogeneous nucleation of a set of very small droplets (pointed by the arrow) induced at the intermediate beam-waist resulting from the lens effect of the nearest beam-trapped droplet. The values of the control parameters are:  $a_0 = 6 \mu\text{m}$ ,  $P_0 = 0.22 \text{ W}$ ,  $T_0 = 298 \text{ K}$ . The bar corresponds to  $50 \mu\text{m}$ .